Differential Effects of Simulated Neural Network's Lesions on Synchrony and EEG Complexity

International Journal of Neural Systems

DIFFERENTIAL EFFECTS OF SIMULATED CORTICAL NETWORK LESIONS ON SYNCHRONY AND EEG COMPLEXITY

ANTONIO JOSÉ IBÁÑEZ-MOLINA*
Department of Psychology, University of Jaén, Jaén, 23071, Spain

SERGIO IGLESIAS-PARRO†
Department of Psychology, University of Jaén, Paraje las Lagunillas s/n, Jaén, 23071, Spain
E-mail: siglesia@ujaen.es
www10.ujaen.es/

JAVIER ESCUDERO‡
School of Engineering, Institute for Digital Communications, University of Edinburgh
Edinburgh, EH9 3FB, United Kingdom
E-mail: Javier.Escudero@ed.ec.uk
www.eng.ed.ac.uk

Brain function has been proposed to arise as a result of the coordinated activity between distributed brain areas. An important issue in the study of brain activity is the characterization of the synchrony among these areas and the resulting complexity of the system. However, the variety of ways to define and, hence, measure brain synchrony and complexity has sometimes led to inconsistent results. Here, we study the relationship between synchrony and commonly used complexity estimators of electroencephalogram (EEG) activity and we explore how simulated lesions in anatomical based cortical networks and the connections between them would affect key functional measures of activity. We explored this question using different types of neural network lesions while the brain dynamics was modelled with a time-delayed set of 66 Kuramoto oscillators. Each oscillator modelled a region of the cortex (node), and the connectivity and spatial location between different areas informed the creation of a network structure (edges). Each type of lesion consisted on successive lesions of nodes or edges during the simulation of the neural dynamics. For each type of lesion, we measured the synchrony among oscillators and three complexity estimators (Higuchi's Fractal Dimension, Sample Entropy and Lempel-Ziv Complexity) of the simulated EEGs. We found a general negative correlation between EEG complexity metrics and synchrony but Sample Entropy and Lempel-Ziv showed a positive correlation with synchrony when the edges of the network were deleted. This suggested an intricate relationship between synchrony of the system and its estimated complexity. Hence, complexity seems to depend on the multiple states of interaction between the oscillators of the system. Our results can contribute to the interpretation of the functional meaning of EEG complexity.

Keywords: Kuramoto model; Network lesions; Synchrony; EEG Complexity

1. Introduction

Major functions of the brain, such as cognitive or emotional processes, have been hypothesized to arise as a result of the transient cooperative activity of distributed but interconnected brain areas [1]. Thus, in order to describe brain functions, it is necessary to unveil the structural and functional interplay between brain regions. One approach to the study of structure-function relationships is to design a mean field model spanning the entire cortical brain functioning[2]. These models allow to manipulate, with high precision, structure and function and measure the changes in their dynamics. It is also possible to use the model to simulate measures as fMRI or EEGs and evaluate experimental measures developed for real patients. In this study, we introduce a neurocomputational model to explore the effects of

*Typeset names in 10 pt Times Roman, uppercase. Use the footnote to indicate the present or permanent address of the author.
†Typeset names in 10 pt Times Roman, uppercase. Use the footnote to indicate the present or permanent address of the author.
‡Typeset names in 10 pt Times Roman, uppercase. Use the footnote to indicate the present or permanent address of the author.

Correspondence autor: ANTONIO JOSÉ IBÁÑEZ-MOLINA anjoibanez@gmail.com

different types of lesions in global brain structure and their consequences at two different levels: (a) general cortical dynamics and (b) the complexity of the simulated EEGs. In this section, we justify these goals by a brief introduction on the effect of structure modification in global brain dynamics; the mean field models as a tool to investigate these dynamics; and the experimental measures of complexity that are able to characterize functional states in real patients.

Understanding the interplay between brain structural networks and function will help us to better comprehend the impact of disease on system's dynamics. Many studies has explored the relationship between synchronicity or neural systems dynamics and different pathologies (e.g., [3–6]). Selectively damaging edges connecting high degree nodes in a magnetoencephalogram (MEG)-derived network has shown to be an effective approach to model the effects of Alzheimer's disease (AD) on brain functional connectivity [7]. Whereas both a targeted lesion and a random error model could account for the decreased level of connectivity in the lower alpha band in AD, only the targeted lesions were able to model the pathophysiological process in that disease [7]. In contrast, cognitive deterioration in normal aging would be regarded as an accumulation of randomly distributed errors [8].

Another fruitful approach to the study of this structure-function interaction is to use neurocomputational models of the entire brain. These models provide functional mechanistic explanations by combining structural information with known dynamical properties of brain networks [9–11]. In general, this approach consists of mean field models (e.g., Kuramoto), which assume that the main dynamics of the neural system can be well approximated by simple, but realistic, network models [12]. Brain dynamics are obtained using a set of coupled non-linear differential equations that describe some key features of the entire working brain. Each differential equation represents a node in the network, which is a dynamical abstraction of the mean activity in a cortical parcellation. Coupling between nodes represents cortical connectivity, which can be experimentally obtained from physiological studies (e.g., diffusion tensor imaging and brain tractography). The dynamics of the models allows simulations of different physiological properties as they are registered with macroscopic measures such as MEGs and EEGs.

Using this methodology, it has been shown that simulated data resembles real brain data when the system exhibits spontaneous phase transitions from order (synchrony between the dynamical elements of the model) to disorder or desynchronization [10]. Networks near such a critical point generate a maximum number of transient states and are especially capable of information processing [13], transmission [14,15] and storage [14,16]. This property of the networks has been designated as metastability [17,18], and is characterized by the tendency of a system of oscillators to continuously migrate between a variety of transient synchronous states, allowing a dynamical organization between the elements of the network. It has been found, for example, that a model of weakly coupled oscillators produce simulated fMRI signals that parallel those from real resting state (endogenous) and focused attention on external events (exogenous) [17], and EEG signals with similar fractal properties to those from mind wandering states from real participants [19].

The above-mentioned studies highlight the importance of the synchronization between elements of brain networks to provide an accurate representation of brain activity. In this vein, synchronization between oscillators has been proposed as a general mechanism for information interchange within neural circuits [20]. Apart from their putative role in normal brain functioning, alterations in neural synchrony parameters have been proposed to be at the root of several mental disorders [21,22]. Thus, disturbed neural synchrony may therefore reflect errors of effective connectivity and neural integration in mental illness [23].

Another important class of measures to characterize brain dynamics are the estimations of the complexity of cortical activity. Cortical complexity is normally estimated with non-linear measures such as fractal dimension or entropy metrics of EEG time series [24–26]. Although non-linear EEG measures have been widely used in the last two decades and they have been useful in the characterization of different brain conditions and diseases [7,27,28] the interpretation of complexity is still controversial. When it is stated, for example, that AD patients exhibit less complex EEG signals than healthy participants [7,27], it would be important to know what this

really means at a neural level. In an early paper, [29] suggested that the fractal dimension of the EEG (measured by correlation dimension, D_2) reflected the number of independent cortical sources in a given period of time. However, later experimental results showed the importance of long-range interactions in cortical dynamics [30,31], suggesting that the concept of independent sources is not appropriate to describe underlying mechanisms of brain signals. Hence, the field shortly started to consider other alternative non-linear metrics, many of which were rooted in the concept of "complexity" [32]. Indeed, the concept of "complexity" can be interpreted in two different ways [28,33]. One notion considers complexity as an intermediate state between randomness and order [33,34]. However, most non-linear metrics applied to brain activity fall within an alternative definition by which complexity is a measure of the degree of randomness or degrees of freedom of a system [32]. Here, we propose that one reliable approach might be to explore variables that contribute to the dynamics of the system as a whole.

With this aim, we utilized a mean field model (i.e., Kuramoto model) to study how structural changes in the network (through directed lesions as well as random errors, both affecting nodes and edges) would modulate the network's dynamics and the complexity exhibited by its simulated EEGs. We developed a computational model that consisted of a set of Kuramoto oscillators with realistic anatomical coupling [35]**.** We calibrated the system so that its dynamics were in a critical point that exhibited a phase transition, since it has been shown that it is a main feature of brain functioning [36]. From this standpoint, then, we tested the effect of lesion changes on the network synchrony with diverse complexity estimators.

2. Methods

2.1. Kuramoto model

2.1.1 Mathematical description

We introduce a modified Kuramoto model [10,37] which consist of a system of coupled differential equations that represent dynamics of N weakly coupled limit-cycle oscillators or rotators with time delays:

$$\frac{\mathrm{d}\theta_i}{\mathrm{dt}} = \omega_i + k\sum_{j=1}^{N} C_{ij}\sin\left(\theta_j\left(t-\tau_{ij}\right)-\theta_i(t)\right), \quad i = 1,\mathrm{K}\ ,N \quad [1]$$

where θ_i is the phase of the i*th* oscillator (i.e., rotator) on its limit cycle and ω_i is its natural frequency ($f_n = \omega_i/2\pi$), drawn from a fixed Gaussian distribution with mean f_0 (f_0=60Hz here) and standard deviation σ_f (σ_f= 1Hz in our analyses). The term C_{ij} is the relative coupling strength from oscillator j to oscillator i (representing the number of fibers between regions, together with the synaptic weights), and k is the global coupling strength which scales all connections' strength. τ_{ij} is the structural conduction delay between the i and j oscillators.

For the Kuramoto model, the overall synchrony of the population of oscillators is conveniently measured by an order parameter (r).

$$r(t) = \left| {}^{1}\!/_{N} \sum_{j=1}^{N} e^{i\theta_j} \right| \quad [2]$$

where $0 \le r(t) \le 1$ measures the phase coherence of the N oscillators, and θ_j is the phase of the oscillator j. If all oscillators are perfectly synchronized with identical angles $\theta_j(t)$, then $r(t) = 1$. In contrast, if all oscillators are spaced equally on the unit circle, then $r(t) = 0$.

The Kuramoto model is a simple model, yet able to simulate macroscopic neural dynamics related to underlying structural connectivity [9,17,38,39]. It has been shown that the Kuramoto model captures aspects of macroscopic dynamics (tens of thousands of simulated neurons) as more complex models [40]. Hence, this model provides a good trade-off between complexity and plausibility [41]. A review can be seen in [42]. Of particular interest here is that the model will undergo a phase transition when the order parameter is in the vicinity of a critical value (k_c). This is important because, according to [43], the behavior of empirical data can be extrapolated from simulated dynamics of an oscillating system at or close to a phase transition.

2.1.2 Implementation of the model

Our model implements 66 Kuramoto oscillators coupled together according to human white matter tractography [35]. Further topological characteristics of the network can be found in [35]. The tractography information is used in our study to determine the length and fiber density between brain regions. The length and fiber density serve as the basis for the elaboration of the

connection strength (**C**) and conduction delay (τ) matrices that give the structural meaning to the network.

Initial conditions of the numerical solution of the model correspond with the first 1000 time steps (100ms) and were discarded from the analyses. For each condition of the study we computed 10 realizations of the model. The model was simulated for 35s in the lesions to nodes conditions, and 40s for the lesions to edges conditions. We used an Euler's integrator scheme with 0.1ms time steps [10]. All simulations were carried out with a mean τ = 3ms and k = 7. These values were chosen because they lead to high metastability and a near-phase transition in the model [36]. After a certain number of steps (detailed in Section 2.3), matrix **C** was modified according to a Targeted Lesion or a Random Error strategy. Thus, the supporting connectivity topology varies through the simulations. All calculations are performed using Matlab®.

2.2. *Network lesions*

This section describes the graph metrics used to characterize the topology and the implementation of the network damages.

2.2.1. *Graph Theory and graph metrics*

In mean-field models of brain functioning, the connections between distant regions of the brain are frequently modeled by a graph whereby the brain is usually parceled in nodes (representing cortical and subcortical areas) connected by edges (representing anatomical or functional connections) [44]. Such graphs constitute a useful tool for studying the complex neuronal structures and their relations. Once a brain graph has been constructed, its topological properties can be measured by a rich collection of metrics [45] [46] providing a common language for the analysis of complex systems.

In the present study, we consider network metrics aimed at describing different properties of the network considering that a waking and conscious brain is the result of two complementary dynamics, namely information integration and differentiation [48]. Thus, we have chosen two graph metrics, commonly used in the field (see for example [49]), that capture these two dynamics: Efficiency and Clustering Coefficient.

We calculated the Efficiency as an indicator of network integration. This is typically quantified with the characteristic path length, which is the average of the shortest path lengths between the nodes, indicating the amount of traffic the network can support [50]. However, we consider the global efficiency as the average inverse shortest path length because the global efficiency may be computed even on disconnected networks [50].

As a complementary measure to Efficiency, we considered the Clustering Coefficient (*CC*), a traditional measure of network segregation [50]. Segregation has been associated with the idea that specialized functions are carried out by clusters of densely interconnected regions. The *CC* assesses segregation by computing the ratio of the number of existing connections to the number of all possible connections in the neighborhood of a node [50]. We compute the mean of the weighted *CC* for all nodes in the network.

2.2.3 Targeted lesions and random errors

We consider both targeted lesions and random errors implemented at the node and edge level, thus leading to four (two by two) different approaches in which the network is damaged. For all conditions, we apply the network lesions while the model is evolving in time so it is possible to evaluate functional changes at many structural states of the network.

As a criterion for node or edge removal in the targeted lesion conditions, we calculate the maximum of the edge and node Betweenness Centrality, which measures the number of shortest paths of the network that go through a particular edge or node [50]. The BC can be interpreted as the amount of control of an edge or node that it has over the communication between elements in the network [51]. Recent work has shown that betweenness-based lesion are more harmful, in terms of altering the communication transmission capacity of the network, than other centrality-based strategies [52]. Hence, the first targeted lesion strategy seeks to damage central nodes of the network. To this end, in each iteration of the deletion process, the node with the highest value of BC is removed from the adjacency matrix. This implies that all connections from and to this node are canceled. For a node h, we made $w_{i,h} = 0$ and $w_{h,j} = 0$, for all i and j. Consequently, the network shrinks in size. This process is repeated until the network contains half the original number of nodes. From a physiological point of view, it has been proposed [53] that node lesions may represent neurodegenerative processes that damage grey matter.

The second targeted lesion strategy damaged central edges to the network. Similarly to the previous case, the edge with the highest value of edge BC is removed from the network in each iteration by making $w_{i,j} = 0$. It must be noted that, in this case, the network does not decrease in size (it is still composed of the same number of nodes). Edge lesions simulate damage to brain white matter [53]. We iterate this process until the number of edges in the network has decreased to half the original number.

Both targeted lesion strategies are deterministic. The order in which nodes and edges are deleted is fixed for a given original topology. However, there is variability in the times at which the lesions or errors occur. We simulate the occurrence of damage to nodes according to a uniform probability density function with limits 5001 and 14999 simulation steps, corresponding to intervals between 0.5s and 1.5s. During our simulations, we consider a far larger number of edge damages. Hence, we simulate the occurrence of an edge damage every *n* simulation steps, with *n* being drawn from a uniform distribution with limits 356 and 996 steps (corresponding to 0.036s and 0.10s). To account for possible effects of initial conditions, simulations were repeated 10 times. Hence, the source of variability in each condition was provided by these realizations.

As a benchmark, we consider two other random eliminations of nodes and edges (random error strategy). In this approach, a randomly selected node (or edge) was removed from the network during realizations of the models. A uniformly distributed random process was selected for node/edge selection. Hence, during random error lesions, the order of node/edge elimination was random. Time intervals between random removals of nodes and edges were the same as above. The elimination process stopped when the number of nodes (or edges) decreased to half the original number. Similarly to the targeted lesion conditions, the simulations were repeated 10 times.

2.3. Simulation of the EEGs

EEG activity from 33 sensors was simulated for the solutions of each model according to the following weighted sum of the activity in each source (oscillator) from the model:

$$x_i(t) = \sum_{j=1}^{N} w_{ij} \sin(\theta_i(t)) + \varepsilon_i(t), \quad i = 1,\text{K}\,,P \qquad [3]$$

where $x_i(t)$ is the time series from sensor *i*th, w_{ij} is the weighted contribution of source *j*th in sensor *i*th. Each w_{ij} was calculated based on a spherical four-shell head model [54] using a standard forward model algorithm[55] . The term $\varepsilon_i(t)$ represents uncorrelated white Gaussian noise added to the signal. In our study, we investigated the effect of noise by adding four levels of intensity.

2.4. Complexity metrics

A number of measures have been proposed to estimate the complexity of EEG signals, but results have not always been convergent [56,57]. Complexity is a term with multiple acceptations[34,58]. The lack of homogeneity in research results can be attributed to different requirements demanded by each measure.

In the context of mental disease, [59] conducted a study in order to compare the discriminative power of several complexity measures. The results showed that Higuchi fractal dimension, Lempel-Ziv complexity and entropy indexes were the more informative to discriminate between schizophrenia patients and controls. Reliable results have been found with these measures in the discrimination of AD patients and controls too [32,60]. In the present study, we aim to explore possible differences in the capability of these measures to capture the effects of different types of lesions on the underlying network dynamics.

2.4.1 Higuchi's Fractal Dimension

The Higuchi's fractal dimension (HFD) is a measure of irregularity and self-similarity of a signal that can be calculated in the time domain [61]. The range of values for HFD lies between 1 and 2, being 1 for a simple curve such as a sine, and 2 for a randomly distributed curve that nearly fills the Euclidean 2D space. HFD has been successfully applied to the analysis of biomedical signals [62,63].

2.4.2 Sample Entropy

Sample Entropy (SampEn) is an irregularity measure defined as a modification of approximate

entropy to reduce its bias, and it is well suited for analyzing short and noisy experimental data [64,65]. SampEn has been successfully applied to EEG analysis in multiple areas (see for example, [31,67–69]).

2.4.3 Lempel-Ziv Complexity

LZC is a widely used metric of complexity in the Kolmogorov's sense [69]. This non-parametric measure assesses the number of distinct substrings and their rate of recurrence along the time series, assigning higher values to more complex data (i.e. higher number of substrings). LZC has been widely applied to biomedical signals [32,70,71] and it has been related to signal concepts such as the bandwidth of random processes and the harmonic variability in quasi-periodic signals [72].

2.4.4 Complexity analysis

HFD, SampEn and LZC are applied to each channel of the simulated EEG signals, which have been band-pass filtered between 2Hz and 80Hz to replicate the process used to select a typical band of interest in EEG analysis. To account for the dependency of the complexity measures on the evolution of the topology of the structural network, we compute the complexity metrics using a sliding window procedure. Successive epochs of the EEGs are selected with a sliding window of 2s (i.e. 2000 samples as the final sampling frequency is 1kHz). This epoch length is similar to that used in other non-linear analysis of electrophysiological brain signals [32]. The sliding windows have 25% overlap. Finally, the complexity metrics are computed within each window and the results are averaged across channels and repetitions of the experiments (type of network damages). We consider global results (averaged over all electrodes).

3. Results

3.1. *Effects of attacks on network topology*

Clustering Coefficient

Once nodes or edges are removed from the network, nodes may become more disconnected from the rest of the network. Clustering coefficient captures these dynamics, being equal to 1 for a node at the center of a fully interlinked cluster, and 0 for a node that is part of a group whose neighbors have no direct connections between them. As can be seen in Figure 1 (bottom panels), the clustering coefficient drop linearly with the random lesions, both for nodes and edges. However, the clustering coefficient behaved differently under targeted lesions. Specifically, for node directed elimination (Figure 1, top left panel) there is an initial fragmentation rate that decreases over lesions until it reaches a minimum value followed by an increase in clustering at the end of the simulation. On the other hand, at the beginning of edge lesions (Figure 1, top right panel), there was a rapid network fragmentation rate followed by a deceleration in the rate of fragmentation.

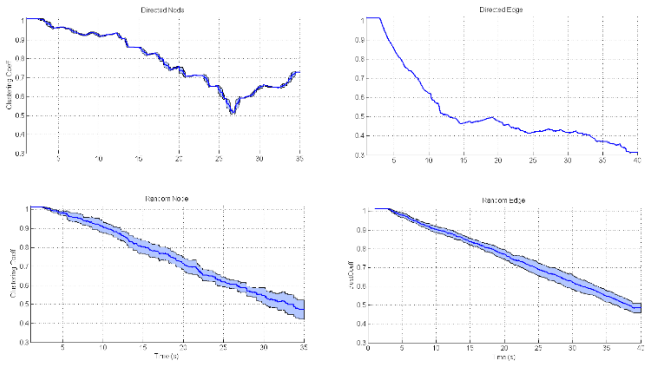

Figure 1. Clustering coefficient values depending on lesion strategy (95% CI shown as shadowed region). Top panels show the effects of directed lesions and low panels show the effects of random lesions.

Efficiency

For each type of lesion, we calculated the evolution of the average inverse shortest path length (efficiency). As can be seen in Figure 2, the loss of the capacity of processing information at the end of the simulation of lesions was similar in all conditions and there was a linear loss of efficiency associated to removals. However, in directed edge elimination, when compared with the other scenarios, there was a quicker initial loss of efficiency, showing again the network vulnerability to selective edge removal.

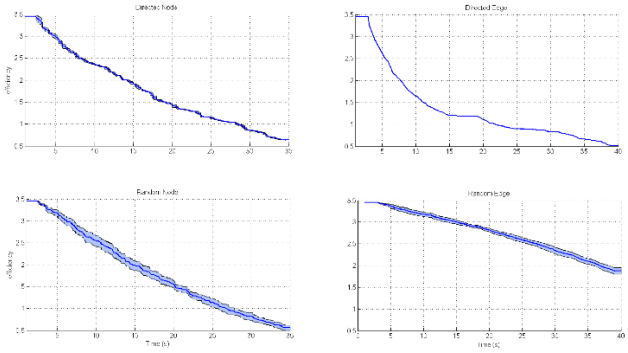

Figure 2. Efficiency values depending on lesion strategy (95% CI shown as shadowed region). Top panels show the effects of directed lesions and low panels show the effects of random lesions

3.2. Effects on synchrony

The order parameter *r* (i.e. synchrony or the coherence among oscillators) is the standard way to describe the collective dynamic of the Kuramoto model. Synchrony has been proposed as a communication mechanism allowing large-scale integration of information [73]. From this point of view, very high or very low levels of synchrony would be seen as indicators of pathological functioning [74].

In Figure 3, we present the average values of *r* for each type of lesion. The system seemed to be more resilient against random errors than to directed lesions. There was a higher loss of synchrony under directed lesions starting about *t*=7s. However, the overall shape of the loss function was similar across conditions.

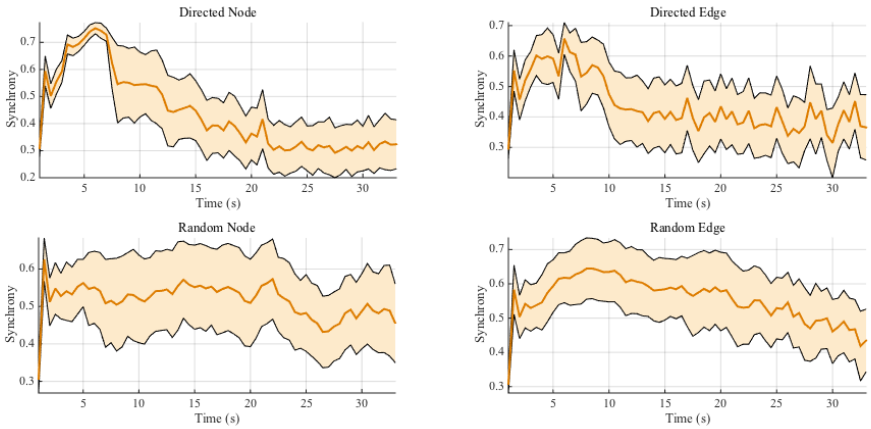

Figure 3. Average values of the Kuramoto's order parameter for each type of lesion (95% CI shown as shadowed region). Top panels show the effects of lesions to nodes and bottom panels show the effects of lesions to edges in the network.

3.3 Effects on EEG complexity

In the following subsections, we present the effects on EEG complexity of random and directed lesions to edges and nodes as they are captured by the different metrics we study (HFD, SampEn and LZC). The reported results reflect the complexity of the whole system by means of an average across all simulated EEG channels.

3.3.1. HFD

Edge Directed Lesions. As can be seen in Figure 4, bottom panels, HFD was relatively unaffected by the presence of noise. The function relating complexity and the edge lesions remained relatively unchanged irrespective of signal to noise ratio. It is interesting to note that the same pattern of robustness against noise could be seen for HFD irrespective of type of lesion. In general, the complexity showed a logarithmic increase with edge directed elimination. That is, HFD suffered a rapid increase followed by a decelerated increase. It should be noted that the edge elimination strategy produced the highest levels of HFD complexity (see Fig.4, third and fourth rows of subplots).

Node Directed Lesions. The network seemed to be more resilient under node directed lesions when compared with edge directed lesions. It took longer (i.e. it requires the elimination of a higher proportion of nodes) to reach similar levels of complexity.

Edge Random Errors. As can be seen in Figure 4, fourth row of subplots, there was a linear increase of the complexity as a function of the increase of edge random failures. The variability of HFD values across simulations increased with the number of failures suggesting more homogeneity in the course of the lesions during the first stages of the elimination process and more heterogeneity following an accumulation of lesions.

Node Random Errors. There was also a linear increase of the complexity as a function of node random errors (see Figure 4, top panels). The system reached similar values of HFD when compared with edge random pruning. The variability of HFD values increased for the lesions produced in the middle of elimination sequence (i.e. lower at the beginning and end and higher in the middle). This condition produced the lowest values of complexity.

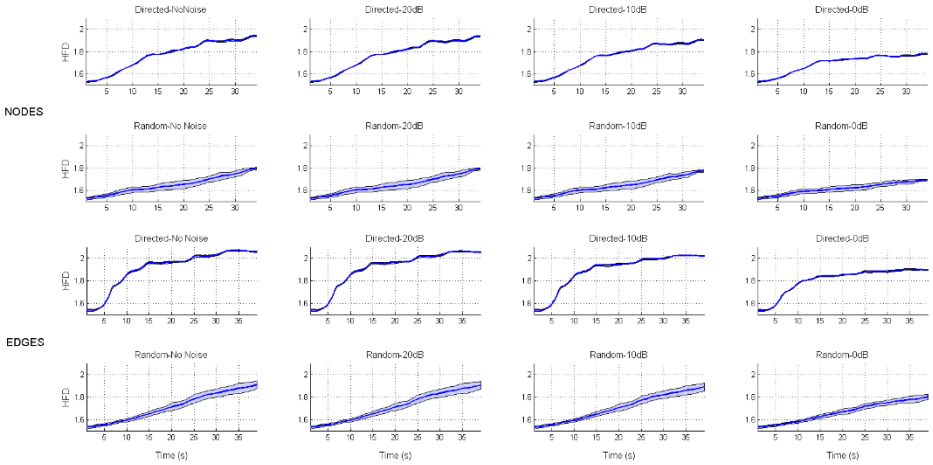

Figure 4. Average values of HFD for each type of lesion and noise level (95% CI shown as shadowed regions). Top panels show HFD for node lesions, and bottom panels show HFD for Edge lesions.

3.3.2. SampEn

Edge Directed Lesions. Relatively unaffected by the presence of noise, the complexity showed a rapid initial increase after which it slightly decreased (for low levels of noise, Fig. 5, bottom panels on the left) or it became stable (for SNR=0dB, Fig. 5, bottom panels on the right).

Node Directed Lesions. There was a rapid increase of the complexity at the beginning of lesions after which SampEn behaved asymptotically. The presence of maximum levels of noise (SNR=0dB) smoothed the growth of complexity (see Fig. 5, first row of subplots on the right).

Edge Random Errors. Relatively unaffected by the presence of noise, after an initial rapid growth of the complexity there was a progressive deceleration of SampEn values (see Fig. 5, third row of subplots).

Node Random Errors. There was an apparent effect of noise on the relationship between complexity and the evolution of failures. Thus, for low noise levels there was a rapid initial increase of the complexity followed by stabilization (see Fig. 5, top panels). However, the increase of noise tends to linearize the relationship between lesions and noise (see Fig. 5, top panels from left to right). There is also a reduction in the variability of complexity as a function of presence of noise. These results might suggest that this level of noise is so high that SampEn is not robust to it anymore and the results are obscured by noise.

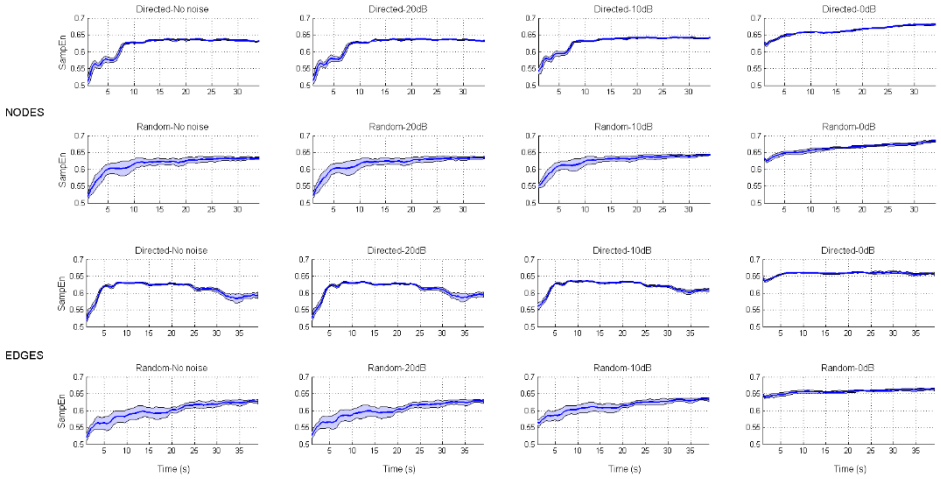

Correspondence autor: ANTONIO JOSÉ IBÁÑEZ-MOLINA anjoibanez@gmail.com

Figure 5. Average values of SampEn for each type of lesion and noise level (95% CI shown as shadowed regions). Top panels show SampEn for node lesions, and bottom panels show SampEn for Edge lesions.

3.3.3. LZC

Edge Directed Lesions. For low to moderate levels of noise (Fig. 6, bottom left panels) the complexity showed an initial increase after which LZC values decreased or it became stable (for SNR=0dB, Fig. 6, bottom panels on the right).

Node Directed Lesions. There is a rapid initial increase of the complexity after which SampEn behaved asymptotically. The presence of maximum level of noise (SNR=0dB) smoothed the growth of complexity (see Fig. 6, top right panels).

Edge Random Errors. In this condition LZC seemed to be relatively unaffected by the presence of noise. There was a monotonically increasing relation between the number of failures and LZC.

Node Random Errors. There was a rapid initial increase of the complexity after which LZC behaved asymptotically (see Fig. 6, top left panels). The presence of maximum level of noise (SNR=0dB) linearized the growth of complexity (see Fig. 6 top right panels).

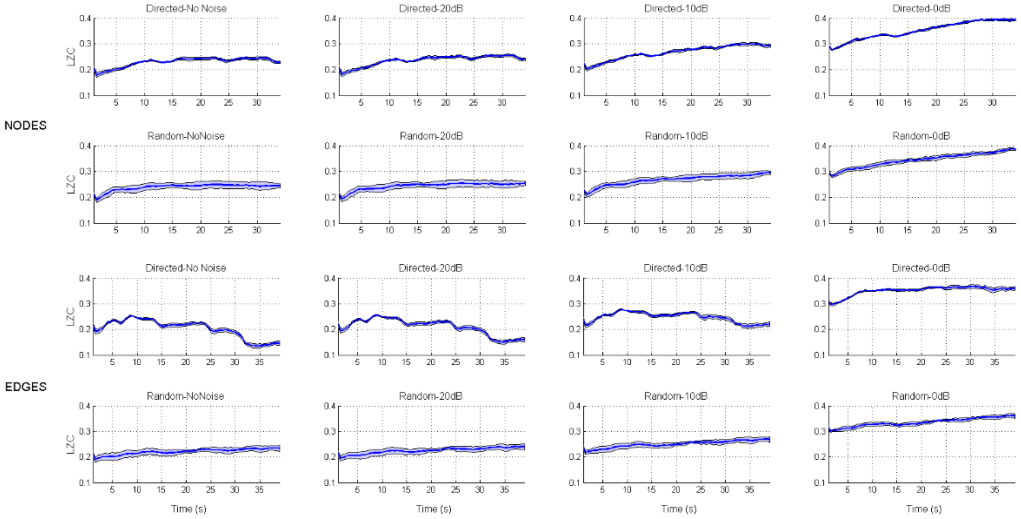

Figure 6. Average values of LZC for each type of lesion and noise level (95% CI shown as shadowed regions). Top panels show LZC for node lesions, and bottom panels show LZC for Edge lesions.

3.3.4. Overview

In sum, HFD showed a general linear progression at most conditions indicating that this measure is sensitive to the number of nodes/edges deleted from the network. However, SampEn and LZC exhibited a different pattern of evolution in complexity during network lesions when compared with HFD. Both SampEn and LZC capture changes in network structure at the beginning of the simulations but reached an approximately stable value until the end of the lesion. This evolution of complexity was stronger for conditions with directed lesions. In addition, SampEn and LZC estimations tend to diminish after the first increase in the condition of edge directed lesions (except for the maximum noise condition).

3.4 Relationship between synchrony and EEG complexity

In order to explore the relationship between complexity and synchrony, the Spearman rank order coefficient was calculated. Due to different length of Node and Edge series, both were resampled. In these analyses, only the complexity metrics of the 12 no-noise conditions were utilized, yielding a 16-order correlation matrix. As can be seen in Figure 7, there were significant positive correlation coefficients between the distinct synchrony measures as well as between most of complexity measures (yellow range). We obtained significant negative correlation coefficients between complexity and synchrony metrics (red range of colors). However, an opposite pattern of results was found for LZC and SampEn measures of complexity in Edge Directed Lesion condition. Specifically, LZC and SampEn showed a significant negative correlation with the other complexity metrics but a significant positive relationship with the synchrony measures.

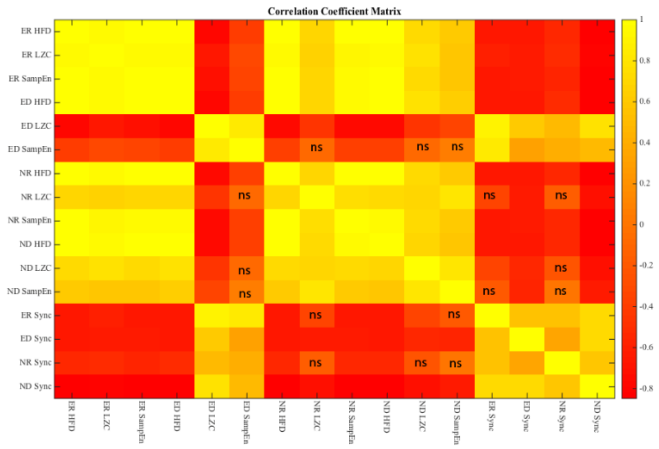

Figure 7. Spearman rank-order correlation calculated among complexity and synchrony measures. Non significant (ns). HFD during Edge Random Errors (ER HFD), LZC during Edge Random Errors (ER LZC), SampEn during Edge Random Errors (ER SampEn), HFD during Edge Directed Lesion (ED HFD), LZC during Edge Directed Lesion (ED LZC), SampEn during Edge Directed Lesion (ED SampEn), HFD during Node Random Errors (NR HFD), LZC during Node Random Errors (NR LZC), SampEn during Node Random Errors (NR SampEn), HFD during Node Directed Lesion (ND HFD), LZC during Node Directed Lesion (ND LZC), SampEn during Node Directed Lesion (ND SampEn), Synchrony during Edge Random Errors (ER Sync), Synchrony during Edge Directed Lesions (ED Sync), Synchrony during Node Random Errors (NR Sync), Synchrony during Node Directed Lesions (ND Sync).

4. Discussion

In this paper, we have considered two interrelated questions: how changes in network structure alter the underlying network functional activity, and how different complexity metrics capture these changes in functional activity. Starting from a structural connectivity network[9,35], we have simulated their oscillatory dynamics using a Kuramoto model [10,37]. From the resulting phases of our Kuramoto oscillators, we calculated the order parameter (*r*, synchrony) in order to summarize the behavior of the whole system. Then, using a standard forward model algorithm [55], cortical EEG activity from 33 sensors was simulated and various measures of signal complexity were obtained (HFD, LZC and SampEn). At that point, we aimed to study how structural changes (node or edge elimination) would impact on function measures (the synchrony among oscillators and the complexity of EEG signals).

Our results showed that the complexity metrics obtained from simulated EEG signals cannot be reduced to a direct relationship with the synchrony of the system, suggesting that the different types of measures that we explored maps onto distinct underlying aspects of system's dynamics.

4.1 Structural connectivity metrics

Random removal of nodes or edges produced a linear reduction in segregation and efficiency. These results replicated observations made by other investigators who examined the robustness of brain networks to random lesions [75–77].

Targeting edges on the basis of their centrality resulted in the rapid appearance of disconnected components and a rapid decrease in the network's global efficiency. On the contrary, targeted removal of nodes with high BC resulted in a more gradual decline in efficiency and fragmentation (comparable to random lesions).

Following a previous study [53], our results may suggest that damages in white mater, particularly in hub regions would have higher impact on integrity and efficiency than damages on grey mater. Moreover, according to Mancini et al. [53] who found greater tolerance to damage in peripheral white mater when compared to damages in hub connections, our results show greater loss of efficiency under edge directed lesions than under node directed lesions. However, these results need to be taken with caution since real brains show a much more intricate pattern of connectivity expanded at several scales, and complementary work need to be conducted to confirm this finding.

4.2. Connectivity and synchrony

Correspondence autor: ANTONIO JOSÉ IBÁÑEZ-MOLINA anjoibanez@gmail.com

Our results showed a general reduction of synchrony tied to lesions irrespective of whether they were random or directed to nodes or edges. These results are in accordance with those obtained by other authors [78] as characteristic of exponential networks. According to these authors, due to the homogeneity of such networks, there is no substantial difference between randomly conducted lesions and those depending on connectivity between its nodes.

In exponential networks, as the proportion of removed elements increases the system's fragmentation increases in a threshold-like fashion (suddenly and fast). In our simulations, even though the 50% of nodes/edges were eliminated, the synchrony did not show an evident transition point in the *r* parameter value whose drop have been indicated a completely loss of the global information-carrying ability of the network. It has been proposed that this robustness to lesions might be due to redundancy in connections [79].

Our data showed a higher loss of synchrony in directed lesions than in random errors. These results contrast with those obtained by [78] who found comparable degree of disconnection for exponential networks either under directed lesions or random errors. Although our connectivity matrix corresponds to an exponential network [35], obtained results would obey the fact that our connectivity matrix is sparse with fiber densities not uniformly distributed across the cortical surface (most of central nodes are located in medial and temporal cortices).

Although transient synchrony between distant areas of the brain seems to be a necessary condition for integration and healthy brain functioning, according to some authors [80,81], brain dynamics cannot be reduced to synchrony, and complexity has been proposed as an additional variable to account for differentiation in brain dynamics [73].

4.3 Complexity measures

Complexity estimators we selected seemed to capture different aspects of the system's dynamics for directed lesions, particularly for edge directed elimination. In this condition, a logarithmic increase in HFD can be observed as a result of central edges elimination, but a different pattern can be observed for SampEn and LZC as lesions occur in time.

Before we continue with the discussion of our results, we may need to consider that what is reflected in the simulated EEGs is a result of the constant adjustment of the phase of each oscillator to synchronize with the rest of them. In addition, the global behavior of the system introduce a general oscillatory activity to EEG data. These two aspects in the dynamics may change complexity in different ways that are not directly predicted from the global synchrony alone. Importantly, these two processes are also observed in studies with real participants where regular oscillatory patterns coexist with irregularities at a different scale. For example, in one study [82], it has been shown that patients with Parkinson exhibit a pathologic interaction between beta oscillations and high frequencies suggesting global-local abnormal interactions in the functional networks of the cortex.

Fractal measures, as HFD, analyze time series at different scales capturing fine grained as well as coarse grained variability. From this point of view HFD captures the whole range of the complexity, and although the physiological nature of fine and coarse time-scales remains unclear [83], it has been proposed that fine time scales maps onto local information processing and coarse time scales maps onto distributed, long range, information processing [84]. From this point of view, HFD might capture changes in information processing at local and at more distributed information processing level.

On the other hand, SampEn is a measure based on Approximate Entropy, and LZC is also considered an entropy related measure closely related to Shannon entropy [69,85]. Both SampEn and LZC indicate the degree of similarity or predictability of time series, where lower values can be found for constant or periodic sequences without any randomness [86]. Moreover, both types of measures are based on a discretization of time series [63,70]. For example, some authors [87] working with heart rate data found that a decrease in the entropy of time series might be due to an increase in the degree of data regularity, or importantly here, it might also be due to the presence of outliers that inflate the observed variance of data. These differential aspects of the measures under consideration might explain the observed differences in our data. Thus, as the central edges are eliminated, the network becomes more fragmented, emerging new communities of oscillators that introduce more variability in the EEG time series reducing in turn the magnitude of entropy-based measures, more sensitive to discretization changes [88]. However, because HFD averages the complexity at different timescales, the loss of complexity

at coarse-grained timescales might be compensated at smaller timescales.

Another important feature in the divergence between HFD and SampEn/LZC is that HFD is not sensitive to stereotypical or repetitive signals. There is no reason why a repetitive signal does not show a high fractal dimension. In other words, one may have predictable time series with a high fractal dimension. Conversely, SampEn and LZC are sensitive to specific oscillatory patterns in the time series, and apparently disordered signals may result less complex if they are constructed with the same sequence patterns. In the case of edge deletion, fragmented groups of oscillators might tend to show more predictable behaviors making the EEG structure simpler in terms of information. When lesions were directed to nodes, EEG variability increases, and then, it is reasonable to consider that the EEG signals may be constructed with less predictable sequences of oscillations that did not decreased the estimation of complexity.

Taking into account these characteristics between the measures, also supported by our data, from a clinical point of view, we might consider the possibility to use HFD in cases where lesions are distributed across scales or they are not well known. In addition, SampEn/LZC could be more suitable for widely distributed pathologies (large scales).

4.3.1. Synchrony and complexity

As a general result, we found an inverse relationship between the degree of neural complexity and phase synchrony between oscillators. These results are in agreement with the [89] proposal of an inverse relationship between complexity and synchrony. According to these authors, signals with more neural complexity establish an environment in which phase relationships are difficult to obtain, thus decreasing the probability of synchrony. Evidences of an inverse relationship between functional connectivity (synchrony) and complexity in brain signals can also be found in other studies [58,83,90]. Nevertheless, and as we mentioned in the previous section, our data also showed that LZC and SampEn in Edge directed lesions tended to decrease in time after an initial increase. This effect explained that LZC and SampEn exhibited a positive correlation with the synchrony of nodes from the network. As suggested before, it was possible that edge deletion left partially isolated groups of oscillators that started to behave more stereotypically; and then, produced more predictable behaviors. This effect might have caused a slight decrease of synchrony/complexity with lesions to edges; and then, a positive correlation between them. It would be equivalent to state that node isolation in the network lead to less synchrony and less informational complexity, but interestingly, as we discussed before, higher estimations of fractal dimension. Hence, there are alternative ways to describe and measure complexity that may lead to divergent results [56,57]. Our results showed how different patterns can be obtained for distinct complexity indexes when applied to the same dataset. Thus, caution should be made in future research when calculating and interpreting complexity measures. Although speculative, our results indicated that is reasonable to expect a HFD and SampEn/LZC divergence when compared with controls for patients with white matter injury (edges), and a high correlation between the three measures for patients with grey matter injury (nodes). For example, it has been shown that white matter degradation is more prominent in Frontotemporal Dementia (FTD) than in AD[91], and therefore it would be reasonable that HFD and SampEn/LZC would show lower positive correlation in FTD than in AD.

4.3.2. Comparison between complexity metrics in terms of their robustness to noise

One of the biggest challenges when using EEG is the very small signal-to-noise ratio of the brain signals that we try to observe. This noise may come from different sources. For example, the variability of individual spike times will result in substantial activity fluctuations when aggregated at the population level [92], providing a "noisy background" which further varies the spike timing [93].

In the present work we have considered 4 different types of network lesions with four different levels of noise each. Complexity measures of random lesions, either to nodes as to edges, seems to be relatively unaffected by SNR. However, in targeted lesions, the increase of noise seems to smooth the increase of complexity. According to various authors [94,95] this robustness may reflect the effect of noise attenuating the relative importance of network elements, either nodes or edges. Thus, although in the directed lesions the nodes/edges were eliminated according to their centrality, the increase of background noise reduces the impact of individual elements on the whole system.

4.3.3. Future research and limitations of the study

Even though we addressed the relationship between whole brain dynamics and the complexity of its generated signals using a well suited mean field model, it is of no doubt that our results are based on a highly abstract model, and the conclusions we extract need to be taken with caution. First, the neural network model the dynamics of only 66 brain regions. This simplification may lead to simple dynamics and hide other possible emerging effects from more complex structures. In addition, the dynamics of the model are based from a narrow frequency band, which obviously, does not correspond with the richness of frequencies we find in real brain functioning. Hence, we believe it would be important to try to replicate our results using larger networks and models that include multiple frequencies.

It would be also important to design experiments to detect divergences between HFD and SampEn/LZC. For example, it would be interesting to compare healthy controls with patients with different types of grey and white matter injury and study the cases in which the pattern of HFD of their EEGs differ from SampEn/LZC estimations.

Finally, one step further of this study will be to design specific lesions in the network that resemble different disorders. One possibility would be to explore Parkinsonism or AD. Since it is well known how the evolution of these pathologies is from a structural point of view, one may model the evolution of the structural network on each pathology and obtain the changes in the corresponding complexity measures.

5. Conclusions

In this study, we modeled brain dynamics using a network of coupled oscillators to investigate directed and random lesions to the network and their effects in synchrony and EEG complexity. Our results showed that HFD increased proportionally with node and edge removal. However, SampEn and LZC tended to increase faster at the beginning and reached a stable value until the end of the lesions. This behavior indicated that these measures, based on information theory, might be sensitive to slight changes in the structure of the system but they could not be appropriate to signals from very disordered systems since the estimations easily reach an asymptotic value. Another finding is that synchrony between oscillators is negatively related with EEG complexity in the majority of conditions we explored; that is, the mean synchrony of the system decreased during network lesions while EEG complexity increased. Although significant, the negative relationship between synchrony and complexity need to be taken into consideration since the evolution curves of synchrony and complexity were different in shape and range of variability (see Figure 7). This can be of interest when we interpret EEG complexity results because in many occasions complexity estimations are thought to reflect de-synchronization or disorder in the system, and we show here that the relationship between the order of the system and the structure of the signal we measure on the scalp is not straightforward.

Acknowledgements

This research was supported by Junta de Andalucía (Biomedical and Heath Science research project PI-0410-2014 and PI-0386-2016).

References

1. Rabinovich, M. I., Simmons, A. N. & Varona, P. Dynamical bridge between brain and mind. *Trends Cogn. Sci.* **19,** 453–461 (2015).
2. Breakspear, M. Dynamic models of large-scale brain activity. *Nat. Neurosci.* **20,** nn.4497 (2017).
3. Ahmadlou, M., Adeli, H. & Adeli, A. Fuzzy Synchronization Likelihood-wavelet methodology for diagnosis of autism spectrum disorder. *J. Neurosci. Methods* **211,** 203–209 (2012).
4. Ahmadlou, M. & Adeli, H. Fuzzy synchronization likelihood with application to attention-deficit/hyperactivity disorder. *Clin. EEG Neurosci.* **42,** 6–13 (2011).
5. Ahmadlou, M. & Adeli, H. Wavelet-synchronization methodology: a new approach for EEG-based diagnosis of ADHD. *Clin. EEG Neurosci.* **41,** 1–10 (2010).
6. Ahmadlou, M. & Adeli, H. Visibility graph similarity: A new measure of generalized synchronization in coupled dynamic systems. *Phys. Nonlinear Phenom.* **241,** 326–332 (2012).
7. Stam, C. J. *et al.* Graph theoretical analysis of magnetoencephalographic functional connectivity in Alzheimer's disease. *Brain* **132,** 213–224 (2009).
8. Rapp, P. R., Deroche, P. S., Mao, Y. & Burwell, R. D. Neuron Number in the Parahippocampal Region is

Preserved in Aged Rats with Spatial Learning Deficits. *Cereb. Cortex* **12,** 1171–1179 (2002).
9. Cabral, J., Hugues, E., Sporns, O. & Deco, G. Role of local network oscillations in resting-state functional connectivity. *NeuroImage* **57,** 130–139 (2011).
10. Cabral, J., Kringelbach, M. L. & Deco, G. Exploring the network dynamics underlying brain activity during rest. *Prog. Neurobiol.* **114,** 102–131 (2014).
11. Honey, C. J., Kötter, R., Breakspear, M. & Sporns, O. Network structure of cerebral cortex shapes functional connectivity on multiple time scales. *Proc. Natl. Acad. Sci.* **104,** 10240–10245 (2007).
12. Deco, G., Jirsa, V. K. & McIntosh, A. R. Emerging concepts for the dynamical organization of resting-state activity in the brain. *Nat. Rev. Neurosci.* **12,** 43–56 (2011).
13. Haldeman, C. & Beggs, J. M. Critical branching captures activity in living neural networks and maximizes the number of metastable States. *Phys. Rev. Lett.* **94,** 058101 (2005).
14. Bertschinger, N. & Natschläger, T. Real-time computation at the edge of chaos in recurrent neural networks. *Neural Comput.* **16,** 1413–1436 (2004).
15. Kinouchi, O. & Copelli, M. Optimal dynamical range of excitable networks at criticality. *Nat. Phys.* **2,** 348–351 (2006).
16. Maass, W., Natschläger, T. & Markram, H. Real-Time Computing Without Stable States: A New Framework for Neural Computation Based on Perturbations. *Neural Comput.* **14,** 2531–2560 (2002).
17. Hellyer, P. J. *et al.* The Control of Global Brain Dynamics: Opposing Actions of Frontoparietal Control and Default Mode Networks on Attention. *J. Neurosci.* **34,** 451–461 (2014).
18. Tognoli, E. & Kelso, J. A. S. The metastable brain. *Neuron* **81,** 35–48 (2014).
19. Ibáñez-Molina, A. J. & Iglesias-Parro, S. Neurocomputational Model of EEG Complexity during Mind Wandering. *Front. Comput. Neurosci.* **10,** (2016).
20. Buzsaki, G. *Rhythms of the Brain*. (Oxford University Press, 2006).
21. Uhlhaas, P. J. & Singer, W. Abnormal neural oscillations and synchrony in schizophrenia. *Nat. Rev. Neurosci.* **11,** 100–113 (2010).
22. Uhlhaas, P. J. & Singer, W. Neuronal Dynamics and Neuropsychiatric Disorders: Toward a Translational Paradigm for Dysfunctional Large-Scale Networks. *Neuron* **75,** 963–980 (2012).
23. Kim, J.-J. *et al.* Functional disconnection between the prefrontal and parietal cortices during working memory processing in schizophrenia: a[15(O)]H2O PET study. *Am. J. Psychiatry* **160,** 919–923 (2003).
24. Ahmadlou, M., Adeli, H. & Adeli, A. Fractality analysis of frontal brain in major depressive disorder. *Int. J. Psychophysiol.* **85,** 206–211 (2012).
25. Ahmadlou, M., Adeli, H. & Adeli, A. Fractality and a wavelet-chaos-methodology for EEG-based diagnosis of Alzheimer disease. *Alzheimer Dis. Assoc. Disord.* **25,** 85–92 (2011).
26. Ahmadlou, M., Adeli, H. & Adeli, A. Improved visibility graph fractality with application for the diagnosis of Autism Spectrum Disorder. *Phys. Stat. Mech. Its Appl.* **391,** 4720–4726 (2012).
27. Jeong, J. EEG dynamics in patients with Alzheimer's disease. *Clin. Neurophysiol. Off. J. Int. Fed. Clin. Neurophysiol.* **115,** 1490–1505 (2004).
28. Stam, C. J. Nonlinear dynamical analysis of EEG and MEG: Review of an emerging field. *Clin. Neurophysiol.* **116,** 2266–2301 (2005).
29. Lutzenberger, W., Preissl, H. & Pulvermüller, F. Fractal dimension of electroencephalographic time series and underlying brain processes. *Biol. Cybern.* **73,** 477–482 (1995).
30. Singer, W. Cortical dynamics revisited. *Trends Cogn. Sci.* **17,** 616–626 (2013).
31. Wolf, F. Symmetry, multistability, and long-range interactions in brain development. *Phys. Rev. Lett.* **95,** 208701 (2005).
32. Hornero, R., Abásolo, D., Escudero, J. & Gómez, C. Nonlinear analysis of electroencephalogram and magnetoencephalogram recordings in patients with Alzheimer's disease. *Philos. Transact. A Math. Phys. Eng. Sci.* **367,** 317–336 (2009).
33. Tononi, G. & Edelman, G. M. Consciousness and Complexity. *Science* **282,** 1846–1851 (1998).
34. Costa, M., Goldberger, A. L. & Peng, C.-K. Multiscale entropy analysis of biological signals. *Phys. Rev. E* **71,** 021906 (2005).
35. Hagmann, P. *et al.* Mapping the Structural Core of Human Cerebral Cortex. *PLoS Biol* **6,** e159 (2008).
36. Escudero, J., Ibanez-Molina, A. & Iglesias-Parro, S. Effect of the average delay and mean connectivity of the Kuramoto model on the complexity of the output electroencephalograms. *Conf. Proc. Annu. Int. Conf. IEEE Eng. Med. Biol. Soc. IEEE Eng. Med. Biol. Soc. Annu. Conf.* **2015,** 7873–7876 (2015).

37. Kuramoto, Y. *Chemical Oscillations, Waves, and Turbulence*. **19,** (Springer Berlin Heidelberg, 1984).
38. Messé, A., Rudrauf, D., Benali, H. & Marrelec, G. Relating Structure and Function in the Human Brain: Relative Contributions of Anatomy, Stationary Dynamics, and Non-stationarities. *PLOS Comput Biol* **10,** e1003530 (2014).
39. Wildie, M. & Shanahan, M. Metastability and chimera states in modular delay and pulse-coupled oscillator networks. *Chaos Woodbury N* **22,** 043131 (2012).
40. Bhowmik, D. & Shanahan, M. Metastability and Inter-Band Frequency Modulation in Networks of Oscillating Spiking Neuron Populations. *PLOS ONE* **8,** e62234 (2013).
41. Hellyer, P. J., Scott, G., Shanahan, M., Sharp, D. J. & Leech, R. Cognitive Flexibility through Metastable Neural Dynamics Is Disrupted by Damage to the Structural Connectome. *J. Neurosci.* **35,** 9050–9063 (2015).
42. Rodrigues, F. A., Peron, T. K. D., Ji, P. & Kurths, J. The Kuramoto model in complex networks. *Phys. Rep.* **610,** 1–98 (2016).
43. Botcharova, M., Farmer, S. F. & Berthouze, L. Power-law distribution of phase-locking intervals does not imply critical interaction. *Phys. Rev. E Stat. Nonlin. Soft Matter Phys.* **86,** 051920 (2012).
44. Bullmore, E. T. & Bassett, D. S. Brain graphs: graphical models of the human brain connectome. *Annu. Rev. Clin. Psychol.* **7,** 113–140 (2011).
45. Erdős, P. & Rényi, A. On the Evolution of Random Graphs. in *PUBLICATION OF THE MATHEMATICAL INSTITUTE OF THE HUNGARIAN ACADEMY OF SCIENCES* 17–61 (1960).
46. Albert, R. & Barabási, A.-L. Statistical mechanics of complex networks. *Rev. Mod. Phys.* **74,** 47–97 (2002).
47. Lee, W. H., Bullmore, E. & Frangou, S. Quantitative evaluation of simulated functional brain networks in graph theoretical analysis. *NeuroImage* **146,** 724–733 (2017).
48. Tononi, G. An information integration theory of consciousness. *BMC Neurosci.* **5,** 42 (2004).
49. Stam, C. J. Modern network science of neurological disorders. *Nat. Rev. Neurosci.* **15,** 683–695 (2014).
50. Rubinov, M. & Sporns, O. Complex network measures of brain connectivity: Uses and interpretations. *NeuroImage* **52,** 1059–1069 (2010).
51. Kivimäki, I., Lebichot, B., Saramäki, J. & Saerens, M. Two betweenness centrality measures based on Randomized Shortest Paths. *Sci. Rep.* **6,** (2016).
52. Holme, P., Kim, B. J., Yoon, C. N. & Han, S. K. Attack vulnerability of complex networks. *Phys. Rev. E Stat. Nonlin. Soft Matter Phys.* **65,** 056109 (2002).
53. Mancini, M. *et al.* Network attack simulations in Alzheimer's disease: The link between network tolerance and neurodegeneration. in *2016 IEEE 13th International Symposium on Biomedical Imaging (ISBI)* 237–240 (2016). doi:10.1109/ISBI.2016.7493253
54. Berg, P. & Scherg, M. A fast method for forward computation of multiple-shell spherical head models. *Electroencephalogr. Clin. Neurophysiol.* **90,** 58–64 (1994).
55. Hoechstetter, K. *et al.* BESA Source Coherence: A New Method to Study Cortical Oscillatory Coupling. *Brain Topogr.* **16,** 233–238 (2004).
56. Koukkou, M., Lehmann, D., Wackermann, J., Dvorak, I. & Henggeler, B. Dimensional complexity of EEG brain mechanisms in untreated schizophrenia. *Biol. Psychiatry* **33,** 397–407 (1993).
57. Lee, Y. J. *et al.* Detection of non-linearity in the EEG of schizophrenic patients. *Clin. Neurophysiol. Off. J. Int. Fed. Clin. Neurophysiol.* **112,** 1288–1294 (2001).
58. Friston, K. J., Tononi, G., Sporns, O. & Edelman, G. M. Characterising the complexity of neuronal interactions. *Hum. Brain Mapp.* **3,** 302–314 (1995).
59. Sabeti, M., Katebi, S. & Boostani, R. Entropy and complexity measures for EEG signal classification of schizophrenic and control participants. *Artif. Intell. Med.* **47,** 263–274 (2009).
60. Gómez, C., Mediavilla, A., Hornero, R., Abásolo, D. & Fernández, A. Use of the Higuchi's fractal dimension for the analysis of MEG recordings from Alzheimer's disease patients. *Med. Eng. Phys.* **31,** 306–313 (2009).
61. Higuchi, T. Approach to an irregular time series on the basis of the fractal theory. *Phys. Nonlinear Phenom.* **31,** 277–283 (1988).
62. Accardo, A., Affinito, M., Carrozzi, M. & Bouquet, F. Use of the fractal dimension for the analysis of electroencephalographic time series. *Biol. Cybern.* **77,** 339–350 (1997).
63. Ibáñez-Molina, A. J. & Iglesias-Parro, S. Fractal characterization of internally and externally generated conscious experiences. *Brain Cogn.* **87,** 69–75 (2014).
64. Pincus, S. M. & Goldberger, A. L. Physiological time-series analysis: what does regularity quantify? *Am. J. Physiol.* **266,** H1643-1656 (1994).
65. Richman, J. S. & Moorman, J. R. Physiological time-series analysis using approximate entropy and sample entropy. *Am. J. Physiol. Heart Circ. Physiol.* **278,** H2039-2049 (2000).
66. Jordan, D., Stockmanns, G., Kochs, E. F., Pilge, S. & Schneider, G. Electroencephalographic order pattern

analysis for the separation of consciousness and unconsciousness: an analysis of approximate entropy, permutation entropy, recurrence rate, and phase coupling of order recurrence plots. *Anesthesiology* **109,** 1014–1022 (2008).

67. Papadelis, C. *et al.* Monitoring sleepiness with on-board electrophysiological recordings for preventing sleep-deprived traffic accidents. *Clin. Neurophysiol. Off. J. Int. Fed. Clin. Neurophysiol.* **118,** 1906–1922 (2007).
68. Yum, M.-K. *et al.* Effect of a ketogenic diet on EEG: analysis of sample entropy. *Seizure* **17,** 561–566 (2008).
69. Lempel, A. & Ziv, J. On the Complexity of Finite Sequences. *IEEE Trans. Inf. Theory* **22,** 75–81 (1976).
70. Fernández, A. *et al.* Lempel-Ziv complexity in schizophrenia: a MEG study. *Clin. Neurophysiol. Off. J. Int. Fed. Clin. Neurophysiol.* **122,** 2227–2235 (2011).
71. Li, Y. *et al.* Abnormal EEG complexity in patients with schizophrenia and depression. *Clin. Neurophysiol. Off. J. Int. Fed. Clin. Neurophysiol.* **119,** 1232–1241 (2008).
72. Aboy, M., Hornero, R., Abásolo, D. & Alvarez, D. Interpretation of the Lempel-Ziv complexity measure in the context of biomedical signal analysis. *IEEE Trans. Biomed. Eng.* **53,** 2282–2288 (2006).
73. Fell, J., Fernández, G. & Elger, C. E. More than synchrony: EEG chaoticity may be necessary for conscious brain functioning. *Med. Hypotheses* **61,** 158–160 (2003).
74. Váša, F. *et al.* Effects of lesions on synchrony and metastability in cortical networks. *NeuroImage* **118,** 456–467 (2015).
75. Achard, S., Salvador, R., Whitcher, B., Suckling, J. & Bullmore, E. A resilient, low-frequency, small-world human brain functional network with highly connected association cortical hubs. *J. Neurosci. Off. J. Soc. Neurosci.* **26,** 63–72 (2006).
76. Alstott, J., Breakspear, M., Hagmann, P., Cammoun, L. & Sporns, O. Modeling the Impact of Lesions in the Human Brain. *PLOS Comput Biol* **5,** e1000408 (2009).
77. Kaiser, M. & Hilgetag, C. C. Edge vulnerability in neural and metabolic networks. *Biol. Cybern.* **90,** 311–317 (2004).
78. Albert, R., Jeong, H. & Barabasi, A.-L. Error and attack tolerance of complex networks : Article : Nature. *Nature* **406,** 378–382 (2000).
79. Anane, R. *et al.* Adaptivity in Heterogeneous EnvironmentsDistributed redundancy and robustness in complex systems. *J. Comput. Syst. Sci.* **77,** 293–304 (2011).
80. Edelman, G. M. & Tononi, G. *A Universe of Consciousness: How Matter Becomes Imagination*. (Basic Books, 2000).
81. Tononi, G., Edelman, G. M. & Sporns, O. Complexity and coherency: integrating information in the brain. *Trends Cogn. Sci.* **2,** 474–484 (1998).
82. López-Azcárate, J. *et al.* Coupling between Beta and High-Frequency Activity in the Human Subthalamic Nucleus May Be a Pathophysiological Mechanism in Parkinson's Disease. *J. Neurosci.* **30,** 6667–6677 (2010).
83. McDonough, I. M. & Nashiro, K. Network complexity as a measure of information processing across resting-state networks: evidence from the Human Connectome Project. *Front. Hum. Neurosci.* **8,** 409 (2014).
84. McIntosh, A. R. *et al.* Spatiotemporal dependency of age-related changes in brain signal variability. *Cereb. Cortex N. Y. N 1991* **24,** 1806–1817 (2014).
85. Cao, Y., Tung, W., Gao, J. B., Protopopescu, V. A. & Hively, L. M. Detecting dynamical changes in time series using the permutation entropy. *Phys. Rev. E* **70,** 046217 (2004).
86. Cover, T. M. & Thomas, J. A. *Elements of Information Theory*. (John Wiley & Sons, 2012).
87. Lake, D. E., Richman, J. S., Griffin, M. P. & Moorman, J. R. Sample entropy analysis of neonatal heart rate variability. *Am. J. Physiol. Regul. Integr. Comp. Physiol.* **283,** R789-797 (2002).
88. Gao, J., Cao, Y., Tung, W. & Hu, J. *Multiscale analysis of complex time series: integration of chaos and random fractal theory, and beyond*. (John Wiley & Sons, 2007).
89. Ghanbari, Y. *et al.* Joint Analysis of Band-Specific Functional Connectivity and Signal Complexity in Autism. *J. Autism Dev. Disord.* **45,** 444–460 (2015).
90. Yang, H., Shew, W. L., Roy, R. & Plenz, D. Maximal Variability of Phase Synchrony in Cortical Networks with Neuronal Avalanches. *J. Neurosci.* **32,** 1061–1072 (2012).
91. Zhang, Y. *et al.* White matter damage in frontotemporal dementia and Alzheimer's disease measured by diffusion MRI. *Brain* **132,** 2579–2592 (2009).
92. Mattia, M. & Del Giudice, P. Population dynamics of interacting spiking neurons. *Phys. Rev. E Stat. Nonlin. Soft Matter Phys.* **66,** 051917 (2002).
93. Braun, J. & Mattia, M. Attractors and noise: twin drivers of decisions and multistability. *NeuroImage* **52,** 740–751 (2010).
94. Basalyga, G. & Salinas, E. When response variability increases neural network robustness to synaptic noise. *Neural Comput.* **18,** 1349–1379 (2006).
95. Faisal, A. A., Selen, L. P. J. & Wolpert, D. M. Noise in the nervous system. *Nat. Rev. Neurosci.* **9,** 292–303 (2008).